Reactions of Laser-Ablated Ruthenium Atoms with CO and H_2 Mixtures: Infrared Spectra and Density Functional Theory Calculations of $H_2Ru(CO)_x$ ($x = 2-4$) and $(H_2)RuCO$

Xuefeng Wang and Lester Andrews*

Department of Chemistry, University of Virginia, McCormick Road, P.O. Box 400319, Charlottesville, Virginia 22904-4319

Received: May 17, 2000; In Final Form: August 14, 2000

Reactions of laser-ablated ruthenium atoms with carbon monoxide and hydrogen in solid argon produce the unsaturated ruthenium carbonyl dihydride $H_2Ru(CO)_2$ and the hydrogen complexes $(H_2)_xRuCO$ ($x = 1, 2$). The observed absorption bands of the reaction products are identified by isotopic substitution and reproduced well by DFT calculations of vibrational fundamentals. The growth of bands due to $H_2Ru(CO)_2$ and (H_2)-RuCO during annealing in solid argon indicates that ruthenium monocarbonyl is coordinated with H_2 to form the dihydrogen complex $(H_2)RuCO$, while $H_2Ru(CO)_2$ is formed from the $(H_2)RuCO$ complex inserting into (H_2) upon coordinating with another CO. Weak bands due to $H_2Ru(CO)_3$ and $H_2Ru(CO)_4$ are also observed.

Introduction

Transition metal hydrides are widely used in a variety of reactions in chemistry, and in particular, are important intermediates in catalytic processes such as hydroformulation,[1] alkane activation reactions,[2−5] and hydrogenation.[6] Similarly, the dihydrogen complexes of transition metals, also known as nonclassical dihydrogen (η^2-H_2) complexes, are of fundamental importance in understanding hydrogenation and the functioning of transition metal containing enzymes,[7] and have been the focus of extensive and continuous study. The first η^2-dihydrogen complexes to be isolated were $M(CO)_3(PR_3)_2(H_2)$, where M = Mo, W and R═Cy, i-Pr.[8,9] Many other nonclassical dihydrogen complexes have been observed in the crystalline state, liquid xenon, the gas phase, and matrix isolation.[10−14] The H_2 elimination or substitution in transition metal hydrides and dihydrogen complexes can provide highly reactive intermediates which can activate dihydrogen or C−H and Si−H bonds in saturated organic compounds (oxidative addition reaction).[15−17]

Nondissociative addition of molecular hydrogen and methane is believed to play an important role in various catalytic processes, for example, in the hydrogenation of olefins. The investigation of reactivity at the transition metal centers of coordinatively unsaturated metal carbonyls is thought to be useful in the elucidation of mechanisms of homogeneous catalytic reactions.[18−24] More recently, various neutral unsaturated metal carbonyls as well as cations and anions are investigated in low-temperature matrix samples by co-deposition of laser ablated transition metal atoms with CO in this laboratory.[25−32] Isotopic substitution and density functional theory frequency calculations can be used to identify reaction products, their electronic states and relative energies. However the reactivity of these species with other small molecules remains unclear. In this work we investigate the reactions of $Ru(CO)_n$ ($n = 1, 2$) complexes with dihydrogen in a low-temperature matrix. The matrix infrared spectroscopic technique is employed to identify the reaction products. The structures, vibrational frequencies, and infrared intensities of the reaction products are confirmed using the effects of isotopic substitution upon the infrared spectra and density functional theory (DFT) calculated frequencies. A reaction mechanism for lower ruthenium carbonyls with dihydrogen is proposed.

* Corresponding author. E-mail: lsa@virginia.edu.

Experimental Section

The experimental methods for reactions of laser-ablated metal atoms with small molecules during condensation in excess argon have been described in detail previously.[33] The Nd:YAG laser fundamental (1064 nm, 10 Hz repetition rate with 10 ns pulse width) was focused onto a rotating pressed ruthenium sponge (Johnson Matthey 99.95%) target. The laser energy was varied from 5 to 20 mJ/pulse. Laser ablated metal atoms were co-deposited with hydrogen (0.05−4.0%) and carbon monoxide (0.05−0.2%) mixtures in argon onto a 7 K CsI window at 2−4 mmol/h for 1 h. Isotopic HD (Cambridge Isotopic Laboratories), D_2(Liquid Carbonic), $^{13}C^{16}O$, and $^{12}C^{18}O$ (Cambridge Isotopic Laboratories) and selected mixtures were used in different experiments. Infrared spectra were recorded at 0.5 cm^{-1} resolution on a Nicolet 750 spectrometer with 0.1 cm^{-1} accuracy using a HgCdTe detector. Matrix samples were annealed at different temperatures, and selected samples were subjected to broadband photolysis by a medium-pressure mercury lamp (Phillips, 175W) with the globe removed.

Results

Experiments were done for laser-ablated Ru atom reactions with CO and H_2 mixtures in argon using low laser energy with different CO and H_2 concentrations. Typical infrared spectra are shown in Figures1−4, and product absorptions are listed in Table 1. The DFT calculations of ruthenium carbonyl dihydrogen complexes and dihydrides are given for assistance in identifying these novel species.

Spectra of Ru Reaction Products. Figure 1 shows the spectra of laser-ablated ruthenium atom co-deposition with 0.5% CO + 2.0% H_2 in argon, and the absorptions are listed in Table 1. After deposition, a weak site split band at 1917.6 and 1923.3 cm^{-1} (RuCO) (Figure 1a) and 1863.4 cm^{-1} (HCO) and 1778.1 cm^{-1} ($RuCO^-$) bands were observed: these bands are characteristic of experiments with CO in argon.[29,34] Annealing to 20

10.1021/jp0018347 CCC: $19.00
Published on Web 10/19/2000

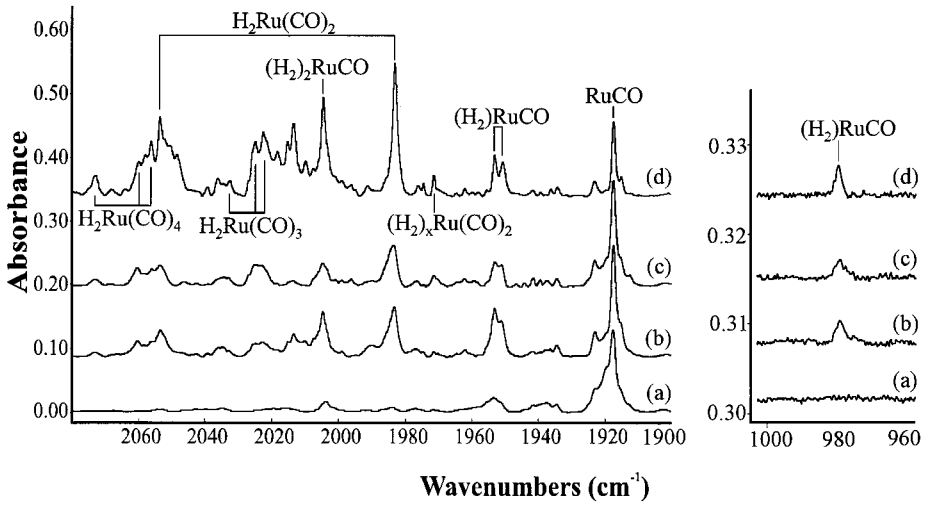

Figure 1. Infrared spectra in 2080−1900 and 1000−960 cm^{-1} regions for laser-ablated Ru atom reaction products with 0.5% CO and 2.0% H_2 in argon during condensation at 7 K: (a) after co-deposition for 60 min, (b) after annealing to 20 K, (c) after 10 min broadband photolysis, and (d) after annealing to 40 K.

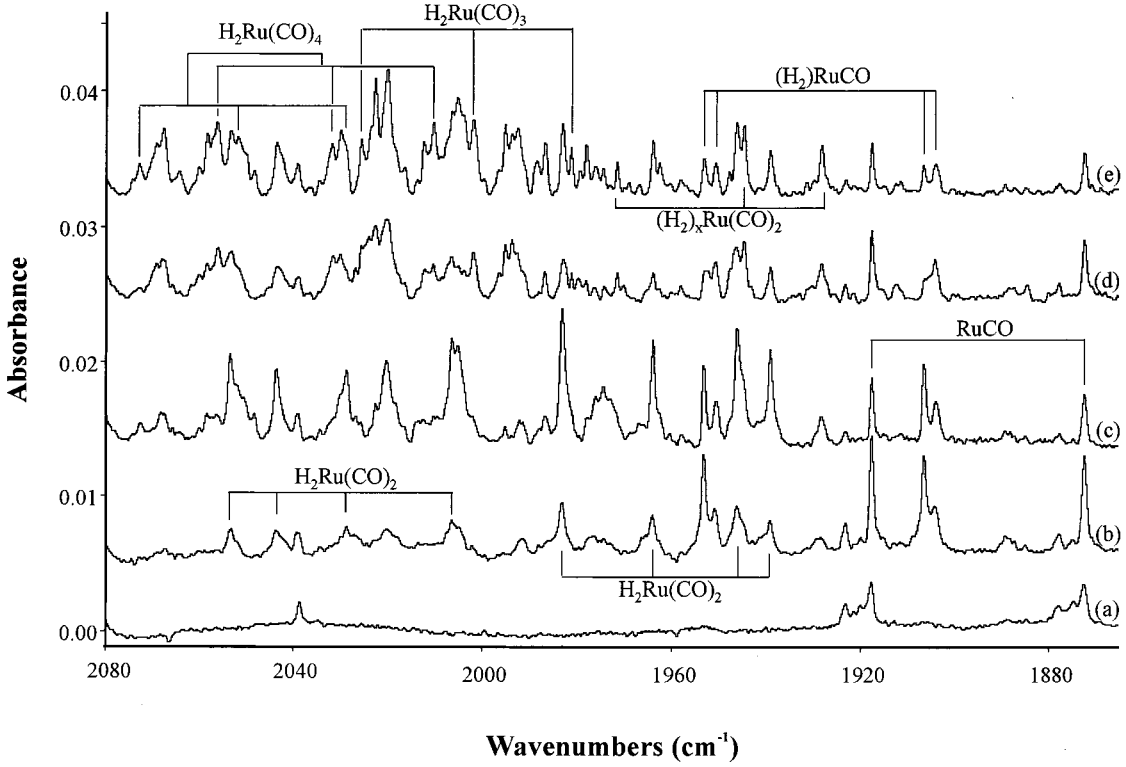

Figure 2. Infrared spectra in 2080−1870 cm^{-1} region for laser-ablated Ru atom reaction products with 0.2% ^{12}CO + 0.2% ^{13}CO + 1% H_2 in argon during condensation at 7 K: (a) after co-deposition for 60 min, (b) after annealing to 20 K, (c) after 10 min broadband photolysis, and (d) after annealing to 40 K.

and 30 K produced new bands at 2072.8, 2060.1, 2056.3, 2053.6, 2036.4, 2022.8, 2004.6, and 1983.2, a new doublet at 1953.2 and 1950.7 cm^{-1}, and a weak band at 978.9 cm^{-1}. The band at 1917.6 cm^{-1} and the 1863.4 and 1778.1 cm^{-1} absorptions increased slightly after annealing. A 10 min broadband photolysis decreased the 2053.6, 1983.2, 1953.2, 1917.6, and 978.9 cm^{-1} absorptions, and destroyed the 1778.8 cm^{-1} band. Further annealing to 35 K greatly increased the 2053.6 and 1983.2 cm^{-1} bands. A final 40 K annealing increased the 2072.8, 2060.1, 2056.3, 2036.4, 2022.8, and 2004.6 cm^{-1} absorptions, and produced a weak new band at 2013.8 cm^{-1}.

For band identification, $^{13}CO/H_2$, $C^{18}O/H_2$, mixed (^{12}CO+^{13}CO)/H_2, $^{12}CO/D_2$, ^{12}CO/HD and mixed $^{12}CO/(H_2+D_2)$ experiments were also performed. Spectra are shown in Figures 2−4 for mixed isotopic samples, and the isotopic absorption bands are listed in Table 1.

Additional experiments with Ru + H_2, HD and D_2 in argon gave only weak bands at 1821.0 and 1312.2 cm^{-1}.

Calculations. Density functional theory (DFT) calculations were performed with the GAUSSIAN 94 program system.[35] Equilibrium geometries were optimized with the density functional BPW91 (Becke exchange with Perdew and Wang correlation); the 6-311+G** basis set for C, O, and H atoms; and LanL2DZ (Los Alamos ECP plus DZ) basis sets for ruthenium;[36−38] such calculations have worked well for transition metal carbonyls.[29−31] Vibrational frequencies were calculated analytically for the fully optimized geometries. The nature of the bonding in the ruthenium carbonyl hydrides and hydrogen

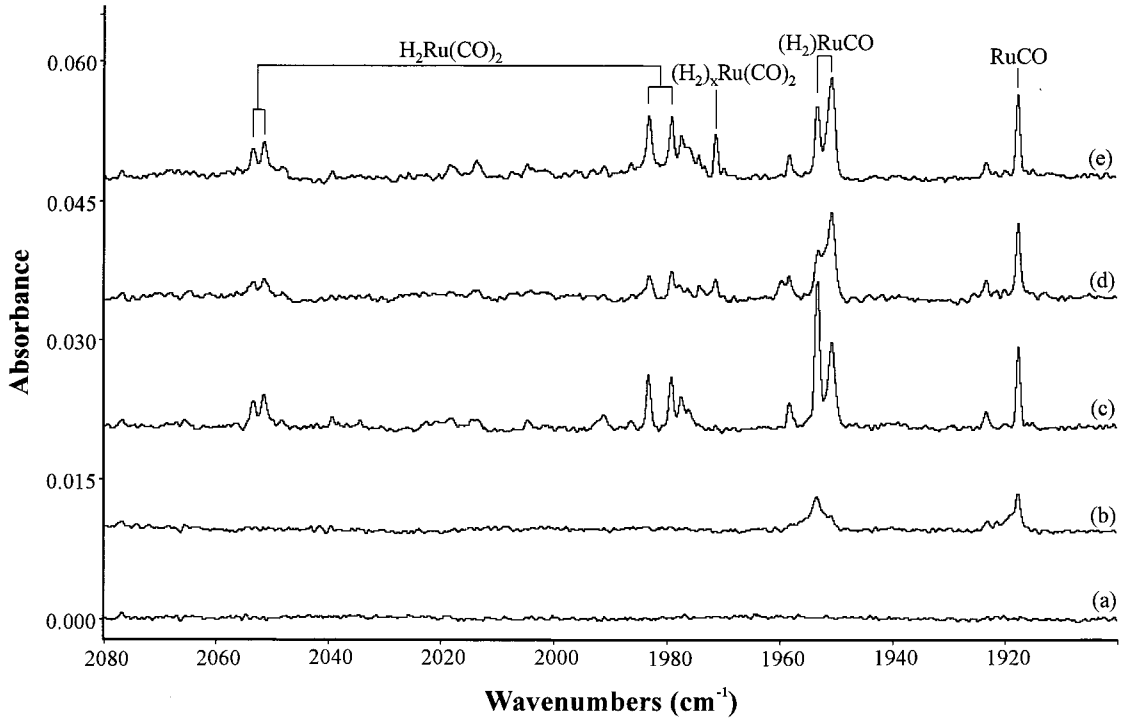

Figure 3. Infrared spectra in the 2080−1900 region for laser-ablated Ru atom reaction products with 0.02% CO + 0.1% H_2 + 0.1% O_2 in argon during condeposition at 7 K: (a) after co-deposition for 60 min, (b) after annealing to 20 K, (c) after annealing to 30 K, (d) after 10 min broadband photolysis, and (e) after annealing to 40 K.

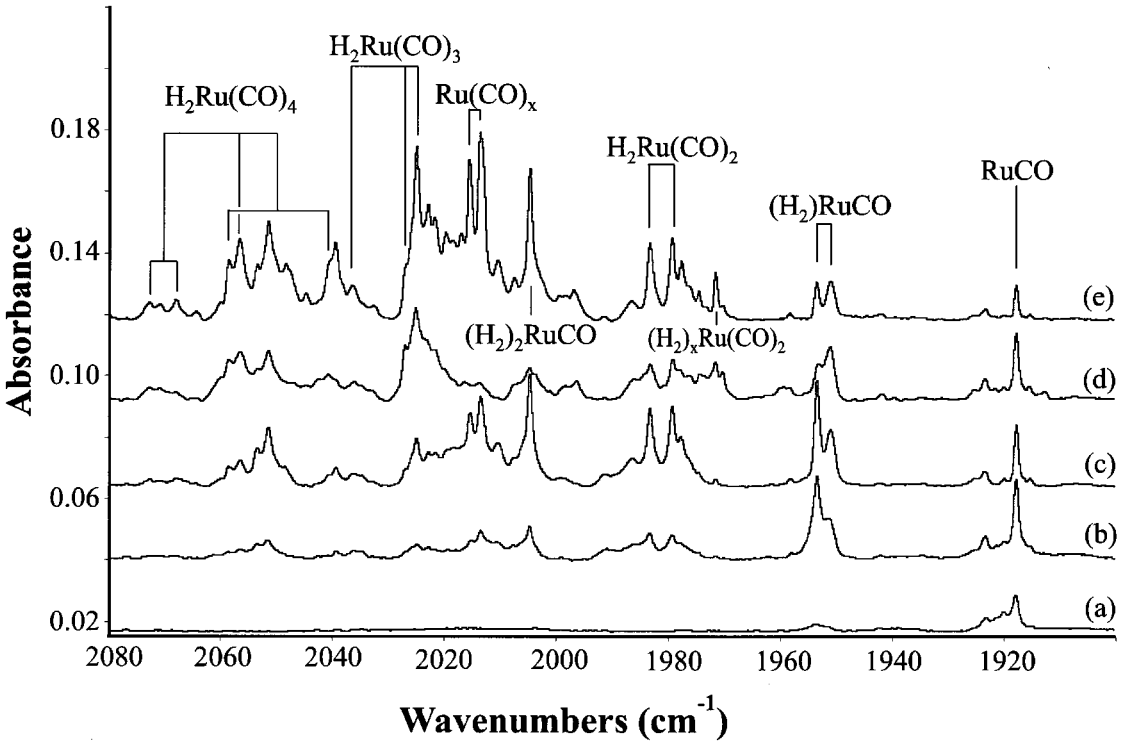

Figure 4. Infrared spectra in 2080−1900 cm^{-1} region for laser-ablated Ru atom reaction products with 0.20% ^{12}CO + 1% H_2 + 1% D_2 in argon during condensation at 7 K: (a) after co-deposition for 60 min, (b) after annealing to 20 K, (c) after 10 min broadband photolysis, and (d) after annealing to 40 K.

complexes was investigated using a natural bond orbital scheme, which has been successfully applied to the analysis of metal−ligand interactions and bonding of metal oxides and nitrides.[39,40] The calculated geometry parameters, total and relative energies, calculated frequencies, and NBO analysis are give in Tables 2−5, respectively.

Four dihydrides, $H_2Ru(CO)_x$ ($x = 1-4$) were calculated, and singlet states were found for all four molecules at this level of theory. The calculated structures are given in Table 2, and several structures are illustrated in Figure 5.

Two equivalent Ru−H bonds were obtained for the H_2RuCO and $H_2Ru(CO)_4$ molecules, but the Ru−H distance in H_2RuCO is 1.559 Å, shorter than in $H_2Ru(CO)_4$ (1.651 Å). However, two inequivalent Ru−H bonds were found in $H_2Ru(CO)_2$ and

TABLE 1: Infrared Absorptions (cm^{-1}) from Co-Deposition of Laser-Ablated Ru Atoms with CO and H_2 Mixtures in Excess Argon

$^{12}CO/H_2$	$^{13}CO/H_2$	$^{12,13}CO/H_2$	$^{18}CO/H_2$	$^{12CO/D}{}_2$	$^{12}CO/(H_2+D_2)$	$^{12}CO/HD$	*R*(12/13)	assignment
2072.8	2027.3		2029.9	2068.0	2072.8, 2068.1	2071.2	1.02244	$H_2Ru(CO)_4$
2060.1	2016.5		2024.6	2040.8	2060.1, 2040.8	2.44.2	1.02162	$H_2Ru(CO)_4$
2056.7	2010.6		2016.9	2056.7	2056.7	2056.6	1.02293	$H_2Ru(CO)_4$
2053.6	2006.6	2053.6, 2043.7, 2028.9, 2006.6	2010.0	2051.4	2053.6, 2051.5	2053.6, 2051.4	1.02342	$H_2Ru(CO)_2$
2036.4	1994.1		1991.6	2026.9	2036.4, 2026.9	2036.4, 2026.9	1.02121	$H_2Ru(CO)_3$
2032.6	1988.3						1.02228	
2025.0	1981.2		1997.7	2024.9	2025.0	2025.0	1.02211	$H_2Ru(CO)_3$
2022.8	1978.1						1.02259	$H_2Ru(CO)_3$
2018.4								$Ru(CO)_x$
2013.8								$(Ru_2(CO)_8)$
2004.6	1960.4						1.02255	$(H_2)_2RuCO$
1983.2	1939.1	1983.2, 1964.0, 1946.1, 1939.1	1941.8	1979.3	1983.2, 1979.2	1984.4, 1979.2	1.02274	$H_2Ru(CO)_2$
1778.1	1737.7	1778.1, 1733.7	1744.1					$RuCO^-$
1971.6	1928.3	1971.6, 1944.6, 1928.4	1924.7		1971.6	1971.4	1.02246	$(H_2)_2Ru(CO)_2$
1953.2	1906.5	1953.2, 1906.5	1913.0	1953.0	1953.1,	1953.2,	1.02439	$(H_2)RuCO$
1950.6	1904.0	1950.6, 1904.0	1910.9	1950.5	1950.7	1950.8	1.02447	site
1923.3	1877.7	1923.3, 1877.7	1882.8	1923.3	1923.3	1923.2	1.02428	RuCO site
1917.6	1872.2	1917.6, 1872.2	1877.4	1917.5	1917.5	1917.6	1.02425	RuCO
1915.2	1871.0		1873.9				1.02362	$Ru(CO)_2$ (linear)
1881.8								$Ru(CO)_4^-$
1863.6	1823.4	1863.4, 1823.3	1818.6			1863.4	1.02205	HCO
1388.2								HO_2
1100.6								HO_2
1085.8						1085.4		HCO
1081.7								site
978.9			978.8			828.2		$(H_2)RuCO$
900.1								RuO

TABLE 2: States, Relative Energies, Dipole Moments, and Geometries Calculated at the BPW91/6-311+G/LANL2DZ Level**

molecules	state	total energy (hartree)	relative energy (kcal/mol)	dipole (debye)	geometry (Å, deg)
RuCO	$^3\Delta$	−207.26007	0.0	3.964	C−O, 1.176; Ru−C, 1.804; ∠RuCO, 180.0
	$^5\sum$	−207.17820	51.4	1.718	C−O, 1.149; Ru−C, 2.157; ∠RuCO, 180.0
	^{1}B	−207.11428	91.5	2.643	C−O, 1.158; Ru−C, 2.019; ∠RuCO, 180.0
$(H_2)RuCO$	$^3A_1$	−208.45423	0.0	3.024	C−O, 1.167; Ru−C, 1.873; Ru−H, 1.884; ∠RuCO, 180.0; ∠HRuH, 24.9
	$^5B_1$	−208.37413	50.3	1.965	C−O, 1.170; Ru−C, 1.950; Ru−H, 1.780; ∠RuCO, 180.0; ∠HRuH, 30.1
	$^1A_1$	−208.29641	99.0	2.903	C−O, 1.157; Ru−C, 2.021; Ru−H, 2.255; ∠RuCO, 180.0; ∠HRuH, 19.4
H_2RuCO	$^1A'$	−208.49105	−23.1	3.849	C−O, 1.174; Ru−C, 1.782; Ru−H, 1.559; ∠RuCO, 180.0; ∠CRuH, 85.8: ∠HRuH, 86.9; ϕ, 94.0
	$^3A''$	−208.44201	7.7	2.627	C−O, 1.167; Ru−C, 1.802; Ru−H, 1.656; ∠RuCO, 180.0; ∠CRuH, 88.5: ∠HRuH, 140.7; ϕ, 94.1
H_4RuCO	$^1A'$	−209.66445		1.404	C−O, 1.159; Ru−C, 1.988; Ru−^{1}H, 1.554; Ru−^{3}H, 1.631; ∠^{1}HRu^{2}H, 59.7; ∠^{3}HRu^{4}H, 69.9;
$Ru(CO)_2$	$^1A_1$	−320.67188	0.0	4.161	C−O, 1.169; Ru−C, 1.806; ∠RuCO, 178.7; ∠CRuC, 86.9
	$^3B_2$	−320.66293	5.6	3.359	C−O, 1.167; Ru−C, 1.881; ∠RuCO, 169.4; ∠CRuC, 101.8
	$^3\Delta_g$	−320.65838	8.5	0.0	C−O, 1.157; Ru−C, 1.962; ∠RuCO, 180.0; ∠CRuC, 180.0
$H_2Ru(CO)_2$	^{1}A	−321.88169	0.0	2.453	^{1}C−^{1}O, 1.156; ^{2}C−^{2}O, 1.164; Ru-^{1}C, 1.985; Ru−^{2}C, 1.808; Ru−^{1}H, 1.556; Ru−^{2}H, 1.650; ∠Ru^{1}C^{1}O, 171.1; ∠Ru^{2}C^{2}O, 178.7; ∠^{1}CRu^{2}C, 98.2 ∠^{1}HRu^{2}H, 82.9; ∠^{1}HRu^{1}C, 89.7; ∠^{1}HRu^{2}C, 85.1; ∠^{2}HRu^{1}C, 172.4; ∠^{2}HRu^{2}C, 79.7;
$(H_2)Ru(CO)_2$	^{1}A	−321.86956	7.6	3.269	^{1}C−^{1}O, 1.168; ^{2}C−^{2}O, 1.161; Ru-^{1}C, 1.804; Ru-^{2}C, 1.897; Ru−^{1}H, 1.827; Ru−^{2}H, 1.745; ∠^{1}HRu^{2}H, 28.3; ∠^{1}CRu^{2}C, 87.8; ∠RuCO, 180;
$(H_2)_2Ru(CO)_2$					
$H_2Ru(CO)_3$ (C_s)	$^1A'$	−435.28418		0.977	RuH, 1.558; RuH′, 1.662; RuC, 1.971; RuC′, 1.945; CO, 1.154; C′O, 1.152; ∠HRuH′, 85.3; ∠HRuC, 89.4; ∠H′RuC′, 80.5; RuCO, 175.3; RuC′O, 173.7
$H_2Ru(CO)_4$ (C_{2v})	$^1A_1$	−548.67393		0.493	C−O, 1.149; C′-O′, 1.150; Ru−C, 1.950; Ru−C′, 1.988; Ru−H, 1.651; ∠HRuH, 82.1; ∠HRuC, 81.2; ∠HruC′, 88.7; ∠RuCO, 11744.5; RuC′O, 180.0
H_4RuCO	$^1A'$	−209.66445		1.404	RuH, 1.554; RuH′, 1.631; RuC, 1.988; CO, 1.159; HRuH, 59.6; H′RuH′, 69.9; RuCO, 169.2

$H_2Ru(CO)_3$. It is interesting to note that for these two molecules the distance of the shorter Ru−H bond is close to that in H_2-RuCO, while the distance of the longer Ru−H bond is similar to that in $H_2Ru(CO)_4$. The bond length of Ru−C in H_2RuCO is 1.782 Å, much shorter than that in $H_2Ru(CO)_4$, while H_2Ru-$(CO)_2$, $H_2Ru(CO)_3$ and $H_2Ru(CO)_4$ have two kinds of inequivalent Ru−C bonds.[41] All four molecules are dihydrides with H−H distances over 2 Å.

Two dihydrogen complexes, namely, $(H_2)RuCO$ and (H_2)-$Ru(CO)_2$, were calculated. The most significant feature of these dihydrogen complexes is that the H−H distance is near the free hydrogen molecule value. Three states, $^3A_1$, $^5B_1$, and $^1A_1$, were considered for $(H_2)RuCO$, and $^3A_1$ was determined to be the ground state. The H−H and Ru−H bond lengths in the $^3A_1$ state are 0.811 and 1.884 Å, respectively, while the H−Ru−H angle is 24.9°. These results indicate that, in the η^2-bonded dihydrogen ruthenium monocarbonyl complex, the H−H bond remains intact with a length just 8% longer than free dihydrogen. The

TABLE 3: Calculated Isotopic C−O Stretching Vibrational Frequencies (cm^{-1}), Intensities (km/mol), and Isotopic Frequency Ratios for $(H_2)Ru(CO)_2$ and $H_2Ru(CO)_2$

molecule	$(^{12}CO)_2$	$(^{13}CO)_2$	HH/$(^{12}CO)_2$	HD/$(^{12}CO)_2$	DH/$(^{12}CO)_2$	DD/$(^{12}CO)_2$	HH/$(^{12}CO)(^{13}CO)$	HH/$(^{12}CO)(^{13}CO)$	HH/$(^{13}CO)_2$	*R*(12/13)
$Ru(CO)_2$	2008.4(361)	1958.6(341)								1.02543
($^1A_1$)	1927.0 (883)	1880.8(835)								1.02456
$Ru(CO)_2$	1974.6(374)	1927.9(355)								1.02422
($^3B_2$)	1916.3(1326)	1872.1(1247)								1.02361
$Ru(CO)_2$	2057.3(0)	2008.1(0)								1.02450
($^3\Delta_g$)	1957.2(2223)	1913.6(2093)								1.02278
$H_2Ru(CO)_2$			2193.5 (19)	2193.0 (20)	2042.4 (440)	2037.7 (381)	2193.5 (18)	2193.5 (19)	2193.5 (18)	1.00000
(^1A)										
			2042.2 (439)	2037.7 (381)	1983.8 (1021)	1978.7 (1005)	2031.5 (570)	2021.3 (417)	1995.7 (449)	1.02330
			1983.7 (1019)	1978.5 (1001)	1875.7 (22.2)	1559.3 (7.4)	1945.9 (843.4)	1962.2 (1006)	1939.4 (923.7)	1.02284
			1874.7 (22)	1339.1 (42)	1558.1 (8)	1338.0 (43)	1874.4 (27)	1870.8 (21)	1870.3 (32)	1.00235
			830.4 (30)	827.0 (21)	768.0 (78)	674.2 (21)	824.1 (31)	830.2 (29)	823.8 (30)	1.00411
			765.8 (69)	660.5 (23)	713.6 (12)	616.6 (29)	765.1 (67)	761.6 (71)	760.9 (70)	1.00644
$(H_2)-Ru(CO)_2$			2660.2 (404)	2344.5 (305)	2306.7 (211)	2023.3 (413)	2660.1 (408)	2660.2 (404)	2660.1 (409)	1.00000
			2021.3 (507)	2019.3 (549)	2020.5 (514)	1950.1 (895)	1999.8 (475)	2008.2 (589)	1972.6 (477)	1.02469
			1950.2 (922)	1950.1 (933)		1879.2 (339)	1925.0 (905)	1915.0 (803)	1903.8 (867)	1.02437
			1600.2 (88)	1324.7 (2.7)	1425.5 (237)	1135.5 (42)	1600.0 (89)	1600.2 (88)	1600.0 (989)	1.00013
			896.9 (255)	785.6 (178)	711.7 (118)	661.4 (101)	896.6 (256)	896.6 (255)	896.3 (256)	1.00067

$(H_2)Ru(CO)_2$ complex ^1A state is located on the potential energy hypersurface. The structure of this species is very similar to its counterpart dihydride $H_2Ru(CO)_2$ except for the η^2-bonded dihydrogen. The H−H bond length in this molecule is 0.877 Å, which is 0.066 Å longer than that in $(H_2)RuCO$. The two hydrogen−ruthenium distances are inequivalent, 1.867 and 1.745 Å, respectively.

The structure and vibrational frequencies of $(H_2)_2RuCO$ are also calculated; the H−H bond lengths are 1.546 and 1.826 Å, and H−Ru−H angles are 59.8° and 69.9°, respectively, while the RuCO is bent with 169.2°. The H−H bond length and H−Ru−H angle are between the hydride and hydrogen complex values.

Discussion

New absorptions will be identified from isotopic shifts and DFT frequency calculations.

$H_2Ru(CO)_2$. The strong bands at 2053.6 and 1983.2 cm^{-1} exhibit the same behavior through deposition, annealing and photolysis experiments, suggesting that they are due to different vibrational modes of the same molecule. Furthermore, these bands require both H_2 and CO in the reaction mixture. When the $^{13}C^{16}O/H_2$ sample was used, the bands shift to 2006.6 and 1939.1 cm^{-1}, confirming that carbon is involved in these modes. The ($^{12}C^{16}O + {}^{13}C^{16}O)/H_2$ sample (^{12}CO:^{13}CO = 1:1) (Figure 2) surprisingly gives 1:1:1:1 quartets for both 2053.6 and 1983.2 cm^{-1} bands. The bands shift to 2051.4 and 1979.3 cm^{-1} (only 2−4 cm^{-1}) in $^{12}CO/D_2$ experiments, as shown in Figure 3 with more diluted sample, indicating that hydrogen is involved in these modes but only to a very limited degree. The 1:1 isotopic doublet shapes with the same frequencies appeared when $^{12}CO/(H_2+D_2)$ and $^{12}CO/HD$ samples were used, indicating only one hydrogen atom is coupled to the C−O vibration. *This evidence suggests that two inequivalent CO groups and possibly one or two hydrogen atoms are bonded to the ruthenium atom.*

Assignment of the above bands to $H_2Ru(CO)_2$ (ruthenium dicarbonyl dihydride) is in excellent agreement with DFT calculations. The BPW91 calculation predicts that $H_2Ru(CO)_2$ is a stable molecule in the ^1A ground electronic state. The H−Ru−H angle is 82.9°, which is close to experimental (87.4°) and theoretical (86.5°) H−Ru−H angle values for $H_2Ru(CO)_4$[41] showing that the two H atoms are completely separated. These results indicate that this molecule is clearly a "classical dihydride", but the two Ru−H bond lengths, 1.556 and 1.650 Å, are not equal although both are shorter than the Ru−H bond length (1.710 Å) in $H_2Ru(CO)_4$.[41] The two carbonyl groups in this molecule are also inequivalent: the longer Ru−C bond (1.985 Å) is very close to the experimental Ru−C bond length (1.974 Å) in the $H_2Ru(CO)_4$ molecule and the shorter Ru−C bond (1.808 C) is almost equal to the bond length of Ru−C (1.806 Å) in $Ru(CO)_2$ ($^1A_1$). The BPW91 calculations gave 2042.2 and 1983.7 cm^{-1} C−O stretching frequencies, which reproduced very well the experimental values (2053.6 and 1983.2 cm^{-1}). The calculated vibrational modes indicate that two C−O stretching modes are weakly coupled with *one* hydrogen atom. As shown in Table 3, the calculated isotopic shifts also agree with experimental results; the two bands red-shift 4.5 and 4.9 cm^{-1} with D_2 substitution. The HD reagent gives two bands, which are almost equivalent to H_2 and D_2 values. Obviously these calculated results match extremely well with the experimental data. The calculations also show that the intensities of the Ru−H vibrations are very weak, and these vibrations are not observed in our spectra.

$(H_2)RuCO$. The absorption band at 1953.2 cm^{-1} and matrix site at 1950.6 cm^{-1} is assigned to $(H_2)RuCO$ (ruthenium

TABLE 4: Calculated Isotopic Vibrational Frequencies (cm^{-1}), Intensities (km/mol), and Isotopic Frequency Ratios for RuCO, $(H_2)Ru(CO)$, $H_2Ru(CO)_3$, and $H_2Ru(CO)_4$

molecule	^{12}CO	^{13}CO	HH/^{12}CO	HH/^{13}CO	HD/^{12}CO	DH/^{12}CO	DD/^{12}CO	*R*(12/13)
RuCO, $^3\Delta$	1933.3(578)	1886.1(549)						1.02503
$^5\Sigma$	2031.4(392)	1986.1(376)						
^1B	2430.5(99)	2372.7(94)						
$(H_2)RuCO\ ^3A_1$			3402.9(353)	3402.8(356)	2953.3(250)		2409.0(137)	1.02421
			1966.8(796)	1920.3(748)	1965.5(815)		1963.1(855)	
			829.9(234)	829.7(234)	678.2(112)		610.0(73)	
$H_2Ru(CO)_3$			2022.4(844)	1979.0(797)	2013.0(794)	2022.4(844)	2013.0(795)	1.02193
			2010.4(1578)	1964.9(1487)	2010.4(1578)	2010.4(1577)	2010.4(1578)	1.02316
$H_2Ru(CO)_4$			2052.6(567)	2007.5(533)	2050.8(591)	2050.8(591)	2046.7(535)	1.02247
			2042.9(902)	2001.5(828)	2035.3(845)	2035.3(845)	2029.3(878)	1.02068
			2040.9(1329)	19945.3(1253)	2040.8(1331)	2040.8(1331)	2040.8(1332)	1.02337
H_4RuCO			2009.6(808)	1973.4(750)			1995.9(681)	1.01834

TABLE 5: Atomic Charge Distributions Based on Natural Population Analysis

	RuCO[a] $^3\Delta$	RuCO $^5\Sigma$	$Ru(CO)_2$[a] $^1A_1$	$Ru(CO)_2\ ^3B_2$	$Ru(CO)_2\ ^3\Delta_g$	$(H_2)RuCO\ ^3A'$	$H_2Ru(CO)_2\ ^1A$
Ru	0.152	0.101	0.014	0.472	0.486	0.146	0.316
^1C	−0.164	−0.00	0.059	−0.146	−0.098	−0.166	0.053
^1O	0.012	−0.097	−0.066	−0.090	−0.146	−0.089	−0.199
^2C			0.059	−0.146	−0.098		−0.038
^2O			−0.066	−0.090	−0.146		−0.123
^1H						0.054	0.061
^2H						0.054	−0.071

[a] Natural electron configurations for RuCO: Ru, 5s(0.75)4d(7.21); C, 2s(1.28)2p(2.29); O, 2s(1.72)2p(4.68) and for $Ru(CO)_2$ Ru, 5s(0.55)4d(7.69); ^1C, ^2C,2s(1.12)2p(2.28); ^1O,^2O, 2s(1.71)2p(4.72).

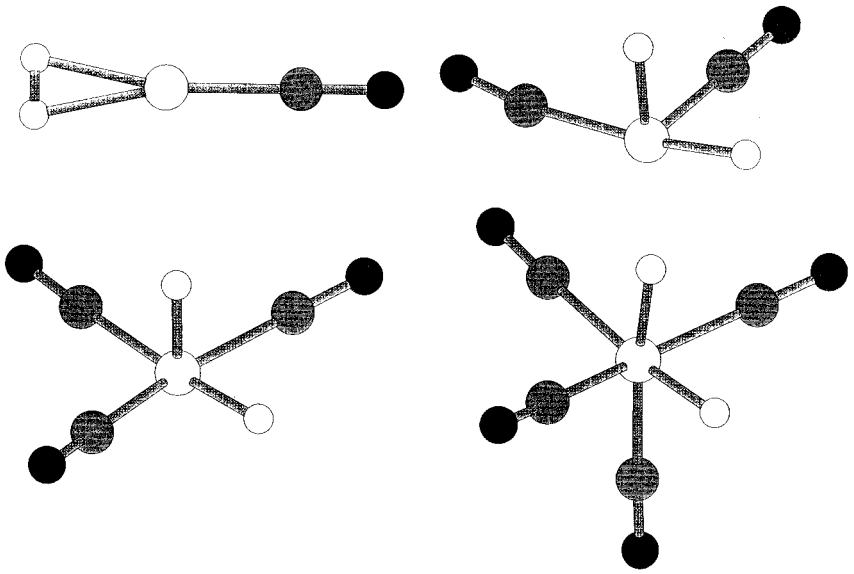

Figure 5. Converged structures and bond lengths (Å) calculated (BPW91/LanL2DZ/6-311+G**) for $^3A_1$ $(H_2)RuCO$, ^1A $H_2Ru(CO)_2$, $H_2Ru(CO)_3$, and $H_2Ru(CO)_4$. Geometric parameters are given in Table 2. The large open circle is Ru.

monocarbonyl dihydrogen complex). Using ^{13}CO this band shifts to 1906.5 cm^{-1} with a $^{12}C/^{13}C$ isotopic ratio of 1.02439. A doublet (1:1) was observed in $^{12}C^{16}O + {}^{13}C^{16}O$ (1:1) experiments, indicating that only one carbonyl is involved. With deuterium substitution the band red-shifted 0.2 cm^{-1}, which indicates that *this vibrational mode involves one CO subunit weakly coupled by a hydrogen molecule.* A weak 978.9 cm^{-1} band tracks with the 1953.2 cm^{-1} band and shows no displacement in ^{13}CO experiments but shifts to 828.2 cm^{-1} with HD and to 704.2 cm^{-1} with D_2.

The above assignments are supported by DFT calculations of vibrational fundamentals for $(H_2)RuCO$. The calculated C−O stretching mode (1966.8 cm^{-1}) and $^{12}CO/^{13}CO$ isotopic ratio (1.02421) agree well with the experimental band at 1953.2 cm^{-1} and the $^{12}CO/^{13}CO$ isotopic ratio of 1.02439. However, we observe a deuterium isotopic blue shift of 0.2 cm^{-1} for this mode, although the calculated red shift is 3.7 cm^{-1}. It appears that the C−O stretching mode is coupled with hydrogen very weakly. The 978.9 cm^{-1} band, which shifted to 828.2 and 704 cm^{-1} in HD and D_2 substituted samples, is assigned as the symmetric (H_2)-Ru stretching mode of the $(H_2)RuCO$ complex. The band is close to this mode in saturated metal carbonyl dihydrogen complexes.[17] The M−H_2 stretching frequency was calculated at 829.9 cm^{-1}, deviating from the experimental value by 15%. Apparently BPW91/6-311+G** calculations underestimate this frequency; however, the use of a larger basis set, aug-cc-PVDZ, for H_2 increased this frequency to 949.3 cm^{-1}, only 3.0% lower than the experimental value. The dihydrogen stretching mode ν(H−H), predicted at 3402.9 cm^{-1} in our calculation, did not appear in the spectrum.

The compounds $M(CO)_3(\eta^2\text{-}H_2)(PR_3)_2$, where M = W, Mo, were first identified by Kubas et al.[8,9] as containing the

molecular hydrogen ligand. These complexes provided the opportunity of studying a new type of chemical hydrogen bond to metals (σ-bond complexes). Previous theoretical studies indicated that for H_2 bound to a metal atom, the interaction consists of a primary donation of electron density from the H−H σ bond to an empty metal orbital and a weak donation of metal d electrons back to the H−H σ^* antibonding orbital.[42,43] The stability of η^2-H_2 complexes depends on the $H_2(\sigma) \rightarrow M(\sigma)$ donation and $M(\pi) \rightarrow H_2(\sigma^*)$ back-donation, both of which weaken the H−H bond. The symmetric M−(H_2) stretching mode has been observed in the IR spectra of 18-electron transition metal dihydrogen complexes[17] in the region 950−850 cm^{-1}. The 978.9 cm^{-1} band assigned to the Ru−(H_2) stretching mode of (H_2)RuCO is slightly higher, reflecting the relative strength of the Ru−(H_2) interaction and a strongly activated H−H bond in this simple dihydrogen complex.

$H_2Ru(CO)_3$. The absorption at 2036.4 cm^{-1} (weaker) and 2025.0 cm^{-1} (stronger) increased together on annealing and broadband photolysis. The 2025.0 cm^{-1} band shifted to 1981.2 cm^{-1} with $^{12}CO/^{13}CO$ isotopic ratios 1.02211, and showed 1:2:1 shape in the mixed $^{12,13}CO + H_2$ experiment. The 2036.4 cm^{-1} band shifted to 1994.1 cm^{-1} with 1.02121 $^{12}CO/^{13}CO$ ratio, and exhibited 1:1 shape in the mixed $^{12,13}CO + H_2$ experiment. The evidence suggests three CO ligands with two equivalent CO subunits in this molecule. The 2036.4 cm^{-1} band shifted to 2026.9 cm^{-1} in CO+D_2 spectra, and showed a 1:1 doublet at 2036.4 and 2026.9 cm^{-1} in both mixed CO + H_2 + D_2 (Figure 4) and CO + HD (not shown) experiments, indicating this CO stretching mode is strongly coupled with hydrogen. However, the 2025.8 cm^{-1} band showed no shift in CO+D_2 and CO + HD experiments. These two bands are assigned to the $H_2Ru(CO)_3$ molecule.

Our DFT calculations further confirmed this assignment and results are summarized in Table 4. The calculations show that the $H_2Ru(CO)_3$ molecule has singlet electronic state with two inequivalent hydrogen atoms. One of the CO stretching modes at 2022.4 cm^{-1} shifts to 2013.0 cm^{-1} for $D_2Ru(CO)_3$ and gives a doublet at 2022.4 and 2013.0 cm^{-1} in $HDRu(CO)_3$, which clearly indicates that this CO stretching mode is strongly coupled with one hydrogen atom in the same plane with one CO subunit with shorter H−Ru bond. However, other symmetric CO stretching mode at 2010.4 cm^{-1} shows no shift in HD and D_2 substituted $H_2Ru(CO)_3$ molecule. The predicted $^{12}CO/^{13}CO$ ratios for two modes match the experimental results very well.

$H_2Ru(CO)_4$. The 2056.7 cm^{-1} band appeared on annealing to 35 K, increased markedly on broadband photolysis and further annealing to 40 K. This band showed no shift in CO+D_2 and CO + HD spectra, but shifted to 2010.6 cm^{-1} with $^{12}CO/^{13}CO$ isotopic ratio 1.02293, and to 2016.9 cm^{-1} in the $C^{18}O$ + H_2 experiment. This band exhibited a triplet pattern in $^{12}CO+^{13}CO$ + H_2 spectra, indicating that two CO subunits are involved. Two other bands at 2072.8 and 2060.1 cm^{-1} track with the 2056.7 cm^{-1} band and the 2072.8 cm^{-1} band also shows triplet in $^{12}CO+^{13}CO$ + Rh spectra. The 2072.8 and 2060.1 cm^{-1} bands shifted to 2068.0 and 2040.8 cm^{-1}, respectively, in CO+D_2 spectra, and both bands showed 1:1 doublet shapes in the CO + H_2 + D_2 experiment and to 2071.2 and 2048.4 cm^{-1} in CO + HD spectra (not shown). These two bands also showed ^{13}CO and $C^{18}O$ shifts; the 2072.8 cm^{-1} band shifted to 2027.3 cm^{-1} with 1.02244 $^{12}CO/^{13}CO$ ratio, and showed triplet pattern in $^{12}CO+^{13}CO$ + H_2 spectra, and the 2060.1 band showed a 1.02162 $^{12}CO/^{13}CO$ isotopic ratio. The 2056.7, 2060.1, and 2072.8 cm^{-1} bands are assigned to the different C−O stretching modes in the $H_2Ru(CO)_4$ molecule with C_{2v} symmetry, respectively.

The 2056.7 and 2072.8 cm^{-1} bands are very close to the observations of Cotton et al. for $H_2Ru(CO)_4$ at 2066 and 2070 cm^{-1} in the gas phase.[44] The DFT calculation of frequencies and vibrational mode assignments for the $H_2Ru(CO)_4$ molecule predicts three very strong symmetric stretching C−O modes, one of which is not, but the other two are coupled with hydrogen. The calculated values are underestimated by 10−20 cm^{-1}, which appear to be a systematic under estimation of C−O stretching modes in ruthenium carbonyl hydrides. However, the predicted isotopic ratios for C−O stretching modes are very close to the experimental results, in which the 12/13 ratio for the uncoupled C−O mode is slightly higher than that for the coupled C−O mode.

$(H_2)_xRu(CO)_2$ and $(H_2)_xRuCO$. A new band at 1971.6 cm^{-1} appears after broadband photolysis. This band increased at the expense of $H_2Ru(CO)_2$. In the $^{13}CO+^{12}CO$ experiments, a triplet (1:2:1) was observed, exhibiting two equivalent carbonyl units. No obvious isotopic shifts were observed in the deuterium experiments. This band is suitable for the antisymmetric vibration of the higher complex $(H_2)_xRu(CO)_2$ molecule.

The dihydrogen ruthenium dicarbonyl complex, $(H_2)Ru(CO)_2$, has been calculated for comparison, and results are summarized in Table 2. The singlet state is 7.6 kcal/mol higher than ground-state $H_2Ru(CO)_2$. The optimized geometry is analogous to the hydride; two carbonyls and two hydrogen atoms are also inequivalent, but the H−Ru−H bond angle of 28.3° indicates a dihydrogen complex. Since no vibrational bands in our spectra match the calculated C−O stretching modes at 1950.2 and 2021.3 cm^{-1} of $(H_2)Ru(CO)_2$, we estimate that the insertion of $Ru(CO)_2$ into the H−H bond has no energy barrier.

A band is observed at 2004.6 cm^{-1} upon deposition and after sample annealing to 20 and 30 K, which diminished on photolysis and recovered on annealing to 35 K. This band was observed weakly with CO (0.2%) + H_2 (0.2%) sample, but enhanced 5 times with CO (0.2%) + H_2 (4%) sample. Clearly higher concentration of hydrogen gives a stronger 2004.6 cm^{-1} band. The ^{13}CO counterpart for this band is 1960.4 cm^{-1} with a $^{12}CO/^{13}CO$ isotopic ratio of 1.02255. Only a 0.2 cm^{-1} blue shift was observed with the CO + D_2 sample. The 1:1 doublet in $^{12}CO/^{13}CO$ experiments suggests only one CO molecule. The DFT predicted CO stretching mode of $(H_2)_2RuCO$ at 2009.6 cm^{-1} is very close to the 2004.6 cm^{-1} experimental value; however, the predicted isotopic shifts of ^{13}CO and D_2 deviate from experiment. Clearly this assignment for the 2004.6 cm^{-1} band is tentative.

Other Products. The laser ablation of ruthenium produces mostly Ru atoms with a small population of Ru^+ and electrons as determined from our study of Ru and CO.[29] On annealing aggregation of metal atoms can occur and weak bands that appear on annealing might be due to dimetal species, but these are difficult to model theoretically. The weak new band that appears at 2013.8 cm^{-1} on annealing is probably due to $Ru_2(CO)_8$.[29] Likewise the 2032.6 cm^{-1} band that appears on annealing is likely due to an unknown aggregate complex that cannot be identified.

The weak bands at 1821.0 cm^{-1} with H_2 and HD and at 1312.2 cm^{-1} with HD and D_2, respectively, are probably due to RuH and RuD. The H/D ratio, 1.3877, is appropriate for a metal hydride diatomic molecule. Our argon matrix RuH absorption is near similar observations of PdH (1953.0 cm^{-1}) and RhH (1920.6 cm^{-1}) in this laboratory.

Bonding Considerations. The trends in the stability of hydrides and η^2-H_2 complexes can be reasoned in term of the molecular orbital description of H_2 bonding to metal centers. The bonding interactions, $H_2(\sigma) \rightarrow M(\sigma)$ donation and $M(\pi) \rightarrow H_2(\sigma^*)$ back-donation are very sensitive to electron density at the metal center. If the metal is electron-rich, the strong back-donation is from the metal to empty antibonding σ^* orbital of H_2 and ultimately facilitates cleavage of the H−H bond to give dihydride complexes. Comparing the natural electron configurations of RuCO and $Ru(CO)_2$ calculated from NBO analysis (Table 5), the 4d population is higher in $Ru(CO)_2$ than that in RuCO, and the ground state $^1A_1$ of $Ru(CO)_2$ has the highest 4d population. This occurs predominantly for the $5s^16d^7$ derived state and is an indication of increased donation from the 5s orbital to the more compact 4d orbital for dicarbonyls. Atomic charge distributions (shown in Table 5) based on Mulliken population analysis indicate that Ru atom in the $^1A_1$ ground-state $Ru(CO)_2$ is more electron-rich compared to the $^3B_2$ and $^3\Delta_g$ states, which have higher positive charges. These charge distributions also indicate that Ru in RuCO is relatively electron-poor compared to Ru in $Ru(CO)_2$. So (H_2)RuCO is stabilized in the argon matrix while the more electron-rich $Ru(CO)_2$ combines with H_2 to give the insertion product.

Reaction Mechanisms. The RuCO intermediate is produced mainly from reaction 1 during deposition with a small contribution from annealing to 20 K. There is growth of RuCO even upon annealing in solid neon at 8 K, so reaction 1 proceeds readily despite the spin change.[29] The further reaction of RuCO with CO is also spontaneous, and $Ru(CO)_2$ is clearly identified in our neon matrix study.[29] As is the case for $Fe(CO)_2$ (see refs 27 and 32), $Ru(CO)_2$ is probably linear in solid neon and bent in solid argon.[29] Reaction 2 is calculated to be exothermic by 47 kcal/mol for the bent dicarbonyl product (BPW91/6-311+G**/LANL2DZ).

$$Ru\ (^5F) + CO(^1\Sigma^+) \rightarrow RuCO(^3\Delta) \qquad \Delta E = -59\ \text{kcal/mol} \quad (1)$$

$$RuCO\ (^3\Delta) + CO(^1\Sigma^+) \rightarrow Ru(CO)_2(^1A_1) \qquad \Delta E = -47\ \text{kcal/mol} \quad (2)$$

However, H_2 is much less reactive with Ru than CO. Although reaction 3 is exothermic by 25 kcal/mol (BPW91/6-311+G*/LANL2DZ), there appears to be a barrier for the insertion of naked atomic Ru into dihydrogen. The reaction of laser-ablated Ru atoms with H_2 in excess argon investigated here found no RuH_2 or $Ru(H_2)$ products; however, with CO present, products containing H_2 were formed.

$$Ru\ (^5F) + H_2(^1\Sigma^+) \rightarrow RuH_2(^3A_2) \qquad \Delta E = -25\ \text{kcal/mol} \quad (3)$$

$$RuCO(^1\Delta) + H_2(^1\Sigma^+) \rightarrow (H_2)RuCO(^3A'') \qquad \Delta E = -11\ \text{kcal/mol} \quad (4)$$

Molecular hydrogen as a dihydrogen ligand coordinated to RuCO was observed in this study, reaction 4, although the dihydride isomer is 23 kcal/mol more stable (Table 2). This suggests that there is an activation energy requirement for insertion of RuCO into dihydrogen, which is apparently not the case for $Ru(CO)_2$. Reaction 4 is computed to be exothermic by 11 kcal/mol. The dihydrogen complexes are usually unstable with respect to H_2 loss. On the basis of electrochemical parameters, thermodynamic data of dihydrogen complexes for the loss of H_2 were reported under 10 kcal/mol in most cases.[45] Obviously the (H_2)RuCO complex has a strong Ru−(H_2) bond, and the slightly high $Ru(H_2)$ stretching vibration supports this conclusion. $H_2Ru(CO)_2$ most likely results from the (H_2)RuCO complex inserting into the dihydrogen ligand upon coordination with another CO, or possibly from the insertion of $Ru(CO)_2$ into the H−H bond, namely the oxidative addition. This is a significant result, as it shows from experimental evidence that the reaction requires little activation energy and is thermodynamically favorable. Reaction 6 is calculated to be exothermic by 21 kcal/mol, which is consistent with the exothermicity of oxidative addition of hydrogen molecule to $Fe(CO)_4$.[46−48]

$$(H_2)Ru(CO)\ (^3A_1) + CO(^1\Sigma^+) \rightarrow H_2Ru(CO)_2 \qquad \Delta E = -57\ \text{kcal/mol} \quad (5)$$

$$Ru(CO)_2(^1A_1) + H_2(^1\Sigma_g^+) \rightarrow H_2Ru(CO)_2(^1A) \qquad \Delta E = -21\ \text{kcal/mol} \quad (6)$$

The reaction 6 should be faster as it is both symmetry and spin allowed. Our DFT calculation predicted that three states ($^1A_1$, $^3B_2$, and $^3\Delta_g$) of $Ru(CO)_2$ molecule very close in energy: $^1A_1$ is the ground state; the $^3B_2$ and $^3\Delta_g$ are respectively 5.6 and 8.5 kcal/mol higher in energy. It is possible that the $(H_2)Ru(CO)_2$ complex is formed from CO bonding to (H_2)RuCO (reaction 5) or H_2 bonding to $Ru(CO)_2$ molecule (Reaction 6), but insertion occurs afterward along the singlet potential energy curve with very small energy barrier. The oxidative addition of H_2 to $Fe(CO)_4$ occurred upon visible irradiation at low temperature.[46] Since the ground state is $^3B_2$ for $Fe(CO)_4$ and $^1A_1$ for $H_2Fe(CO)_4$, it is believed that the reaction proceed with 10 kcal/mol energy barrier on the basis of spin−orbit coupling consideration.[47] The reaction 5 is presumed to take place without C_{2v} constraint from the calculated molecular structures of hydrogen complex $(H_2)Ru(CO)_2$ and insertion product $H_2Ru(CO)_2$. The structural parameters as listed in Table 2 show that both molecules are unfavorable for C_{2v} symmetry structures. We believe that the oxidative addition of H_2 to $Ru(CO)_2$ is allowed with much lower energy barrier than the reaction H_2 and $Fe(CO)_4$.

The photochemical reverse reaction observed after 254 nm irradiation of $H_2Ru(CO)_2$ is reductive elimination of molecular hydrogen. This reaction is analogous to the reductive elimination of H_2 from general photochemically induced reactions of transition metal dihydrides with a variety of ligands. The $Ru(CO)_2$ molecule is highly reactive, and it can be stabilized with other ligands in the argon matrix, most probably recombining with two H_2 molecules.

$$H_2Ru(CO)_2(^1A) \xrightarrow{254\ \text{nm}} H_2 + Ru(CO)_2(^1A_1) \quad (7)$$

$$Ru(CO)_2 + xH_2 \rightarrow (H_2)_xRu(CO)_2 \quad (8)$$

$H_2Ru(CO)_3$ and $H_2Ru(CO)_4$ are produced on further annealing as other CO ligands are added to the unsaturated $H_2Ru(CO)_2$ complex, reactions 9 and 10.

$$H_2Ru(CO)_2 + CO \rightarrow H_2Ru(CO)_3 \qquad \Delta E = -41\ \text{kcal/mol} \quad (9)$$

$$H_2Ru(CO)_3 + CO \rightarrow H_2Ru(CO)_4 \qquad \Delta E = -34\ \text{kcal/mol} \quad (10)$$

Conclusions

The unsaturated ruthenium carbonyl dihydrogen complexes and ruthenium carbonyl dihydrides have been characterized by

matrix isolation infrared spectroscopy. Reactions of laser-ablated ruthenium atoms with CO and H_2 mixtures during co-deposition, and further reactions on annealing and photolysis produced $(H_2)RuCO$, $H_2Ru(CO)_2$, $H_2Ru(CO)_3$, and saturated $H_2Ru(CO)_4$. It is clear from these experiments that Ru first reacts with CO and then with H_2. New bands at 2053.6 and 1983.2 cm^{-1} increased on sample annealing but disappeared on photolysis, and are assigned to the unsaturated $H_2Ru(CO)_2$ complex based on ^{13}CO, $C^{18}O$, HD and D_2 isotopic shifts, and the spectra of isotopic mixtures. The bands at 1953.2 and 978.9 cm^{-1} are assigned to the dihydrogen complex, $(H_2)RuCO$. The observed spectra are reproduced well by DFT/BPW91 frequency calculations. The $H_2Ru(CO)_3$ and $H_2Ru(CO)_4$ complexes were also produced on annealing and photolysis, and identified from isotopic shifts and DFT calculations.

The $H_2Ru(CO)_2$ dihydride complex most likely results from the $(H_2)RuCO$ complex inserting into the dihydrogen ligand upon coordination with another CO, or possibly from the direct insertion of $Ru(CO)_2$ into the H−H bond. Our observations suggest that the reaction of $RuCO_2$ with H_2 requires little activation energy and is thermodynamically favorable.

Acknowledgment. We acknowledge support for this research from the National Science Foundation and the Air Force Office of Scientific Research.

References and Notes

(1) Sanchez-Delgado, R. A.; Bradley, J. S.; Wilkinson, G. *J. Chem. Soc., Dalton Trans*. **1976**, *5*, 399.
(2) Crabtree, R. H.; Dion, R. P. *J. Chem. Soc., Chem. Commun*. **1984**, *19*, 1260.
(3) Burk, M. J.; Crabtree, R. H.; Parnell, C. P.; Uriarte, R. J. *Organometallics* **1984**, *3*, 816.
(4) Crabtree, R. H. *Chem. Rev.* **1985**, *85*, 245.
(5) Stoutland, P. O.; Bergman, R. G.; Nolan, S. P.; Hoff, C. D. *Polyhedron* **1988**, *7*, 1429.
(6) Harris, R. O.; Hota, N. K.; Sadavoy, L.; Yuen, J. M. C. *J. Organomet. Chem*. **1973**, *54*, 259.
(7) Adams, M. W. W.; Mortenson, L. E.; Chen, J. S. *Biochim. Biophys. Acta* **1981**, *105*, 594.
(8) Kubas, G. J.; Ryan, R. R.; Swanson, B. I.; Vergamini, P. J.; Wasserman, H. J. *J. Am. Chem. Soc*. **1984**, *106*, 451.
(9) Kubas, G. J. *Acc. Chem. Res*. **1988**, *21*, 120.
(10) (a) Upmacis, R. K.; Poliakoff, M.; Turner, J. J. *J Am. Chem. Soc*. **1986**, *108*, 3645. (b) Gadd, G. E.; Upmacis, R. K.; Poliakoff, M.; Turner, J. J. *J. Am. Chem. Soc*. **1986**, *108*, 2547. (c) Jackson, S. A.; Hodges, P. M.; Poliakoff, M.; Turner, J. J.; Grevels, F. W. *J. Am. Chem. Soc*. **1990**, *112*, 1221.
(11) Crabtree, R. H.; Lavin, M.; Bonneviot, L. *J. Am. Chem Soc*. **1986**, *108*, 4032.
(12) Jia, G.; Meek, D. W. *J. Am. Chem. Soc*. **1989**, *111*, 757.
(13) Mediati, M.; Tachibana, G. N.; Jensen, C. M. *Inorg. Chem*. **1990**, *29*, 3.
(14) Hampton, C.; Cullen, W. R.; James, B. R.; Charland, J. P. *J. Am. Chem. Soc*. **1988**, *110*, 6918.
(15) Dedieu, A., Ed. *Transition Metal Hydrides*; VCH Publishers: NewYork, 1991.
(16) Jessop, P. G.; Morris, R. H. *Coord. Chem. Rev*. **1992**, *121*, 155.
(17) Eckert, J. *Spectrochim. Acta* **1992**, *48A* 363.
(18) Janowiz, A. H.; Bergman, R. G. *J. Am. Chem. Soc*. **1982**, *104*, 352.
(19) Wenzel, T. J.; Bergman, R. G. *J. Am. Chem. Soc*. **1986**, *108*, 4856.
(20) Fisher, B. J.; Eisenberg, R. *Organometallics* **1983**, *2*, 764.
(21) Wu, J.; Bergman, R. G. *J. Am. Chem. Soc*. **1989**, *111*, 7628.
(22) Peerlans, R. A.; Bergman, R. G. *Organometallics* **1984**, *3*, 508.
(23) (a) Wink, D. A.; Ford, P. C. *J. Am. Chem. Soc*. **1985**, *107*, 5566. (b) Wink, D. A.; Ford, P. C. *J. Am. Chem. Soc*. **1986**, *108*, 4838.
(24) Crabtree, R. H. *Acc. Chem. Res*. **1990**, *23*, 95.
(25) Zhou, M. F.; Andrews, L. *J. Am. Chem. Soc*. **1998**, *120*, 11499 (Ni + CO).
(26) Zhou, M. F.; Andrews, L. *J. Phys. Chem. A* **1999**, *103*, 2964 (Sc + CO).
(27) Zhou, M. F.;. Chertihin, G. V.; Andrews, L. *J. Chem. Phys*. **1998**, *109*, 10893 (Fe + CO).
(28) Zhou, M. F.; Andrews, L. *J. Phys. Chem. A* **1999**, *103*, 5259 (V, Ti + CO).
(29) Zhou, M. F.; Andrews, L. *J. Phys. Chem. A* **1999**, *103*, 6956 (Ru, Os + CO).
(30) Zhou, M. F.; Andrews, L. *J. Phys. Chem. A* **1999**, *103*, 7773 (Co, Rh, Ir + CO).
(31) Zhou, M. F.; Andrews, L. *J. Phys. Chem. A* **1999**, *103*, 7785 (Nb, Ta + CO).
(32) Zhou, M. F.; Andrews, L. *J. Chem. Phys*. **1999**, *110*, 10370 (Fe + CO).
(33) Burkholder, T. R.; Andrews, L. *J. Chem. Phys*. **1991**, *95*, 8697. Hassanzadeh, P.; Andrews, L. *J. Phys. Chem*. **1992**, *96*, 9177.
(34) Milligan, D. E.; Jacox, M. E. *J. Chem. Phys.* **1969**, *51*, 277.
(35) Frisch, M. J.; Trucks, G. W.; Schlegel, H. B.; Gill, P. M. W.; Johnson, B. G.; Robb, M. A.; Cheeseman, J. R.; Keith, T.; Petersson, G. A.; Montgomery, J. A.; Raghavachari, K.; Al-Laham, M. A.; Zakrzewski, V. G.; Ortiz, J. V.; Foresman, J. B.; Cioslowski, J.; Stefanov, B. B.; Nanayakkara, A.; Challacombe, M.; Peng, C. Y.; Ayala, P. Y.; Chen, W.; Wong, M. W.; Andres, J. L.; Replogle, E. S.; Gomperts, R. R.; Martin, L.; Fox, D. J.; Binkley, J. S.; Defrees, D. J.; Baker, J.; Stewart, J. P.; Head-Gordon, M.; Gonzalez, C.; Pople, J. A. *Gaussian 94*, Revision B.1; Gaussian Inc.: Pittsburgh, PA, 1995.
(36) Perdew, J. P. *Phys. Rev. B* **1986**, *33*, 8822.
(37) Becke, A. D. *J. Chem. Phys*. **1993**, *98*, 5648.
(38) Hay, P. J.; Wadt, W. R. *J. Chem. Phys*. **1985**, *82*, 299.
(39) Reed, A. E.; Curtiss, L. A.; Weinhold, F. *Chem. Rev*. **1988**, *88*, 899.
(40) (a) Citra, A.; Andrews, L. *J. Phys. Chem. A* **1999**, *103*, 4182. (b) Citra, A.; Andrews, L. *J. Phys. Chem. A* **2000**, *104*, 1152.
(41) Lavaty, T. G.; Wikrent, P.; Drouin, B. J.; Kukolich, S. G. *J. Chem. Phys*. **1998**, *109*, 9473.
(42) Lin, Z. Y.; Hall, M. B.; *J. Am. Chem. Soc*. **1992**, *114*, 6102.
(43) Verslius, L.; Ziegler, T.; *Organometallics* **1990**, *9*, 2985.
(44) Cotton, J. D.; Bruce, M. I.; Stone, F. G. A. *J. Chem. Soc. A* **1968**, 2162.
(45) (a) Lever, A. B. P. *Inorg. Chem*. **1990**, *29*, 1271. (b) Lever, A. B. P. *Inorg. Chem*. **1991**, *30*, 1980.
(46) Sweany, R. L. *J. Am. Chem. Soc.* **1981**, *103*, 2410.
(47) Daniel, C. *J. Phys. Chem*. **1991**, *95*, 2394.
(48) Heitz, M. C.; Daniel, C. *J. Am. Chem. Soc*. **1997**, *119*. 8269.